Simulation Study of Microwave Imaging for Brain Disease Diagnostic

Stephanie Sia Sok San[1], Mohd Hafiz Fazalul Rahiman[1], Zulkarnay Zakaria[1], Masturah Tunnur Mohd Talib[1], Jaysuman Pusppanathan[2] and Juliza Jamaludin[3]
[1]*Tomography Imaging and Instrumentation Research Group, School of Mechatronic Engineering, Universiti Malaysia Perlis, Pauh Putra Campus, 02600 Arau, Perlis, Malaysia.*
[2]*Faculty of Biosciences & Medical Engineering, Universiti Teknologi Malaysia, 81310 Skudai Johor, Malaysia.*
[3]*Faculty of Engineering and Built Environment, Universiti Sains Islam Malaysia, 71800 Bandar Baru Nilai, Negeri Sembilan, Malaysia*
hafiz@unimap.edu.my

***Abstract*—Brain tumour result by abnormal growth and division of cell inside the skull show high potential to become malignancies and lead to brain damage or even death. Early detection is crucial for further treatment to increase the survival rate of patients who have brain cancer. Existing clinical imaging possess limitation as they are costly, time-consuming and some of them depend on ionising radiation. The microwave imaging has emerged as the new preliminary diagnosis method as it is portable, non-ionising, low cost, and able to produce a good spatial resolution. This paper will be discussing the microwave head based sensing and imaging techniques for brain tumour diagnosis. The 2D FEM approach is applied to solve the forward problem, and the image is reconstructed by implementing linear back projection. Eight rectangular sensing electrodes are arranged in an elliptical array around the head phantom. When one electrode is transmitting the microwave, the remaining of the electrode served as the receiver. The different tumour position is simulated to test the reliability of the system. Lastly, the system is able to detect the tumour, and 1 GHz is chosen as the best frequency based on the simulation and image reconstructed.**

***Index Terms*— Brain Tumour; Finite Element Modelling; Linear Back Projection; Microwave Imaging**

I. INTRODUCTION

Brain disease diagnosis can be categorised into a various form which includes infection, trauma, stroke, seizure, and tumour. Studies showed that a brain tumour had become the second leading cause of death in cancer between the age of 0-19 in the U.S. and Canada [1]. The most common medical modality for brain tumour diagnosis is computerised tomography scan (CT scan), magnetic resonance (MRI), and Positron Emission Tomography (PET).

Although CT scan is the primary diagnosis for the brain disease, it involves of the usage of X-ray to create the detail of the head tissue. Excess of exposure to radiation will poses health risk to the patient seven develop cancer [2]. Modalities such as MRI is considered as one of the safest medical imaging techniques which operate without expose to the ionising radiation. However, it is expensive and cannot be accessed in the rural area. Some of the people will experience claustrophobic due to being placed in an enclosed space while having an MRI scan. Besides that, the strong magnetic field may also give an effect on the patient with an implantable cardiac pacemaker as an example. Hence Microwave Imaging (MWI) has been suggested as a candidate for new medical imaging diagnosis as it is non- invasive, free ionising radiation, cost-efficient and safe to be used.

Microwaves can penetrate through different mediums for example soil, wood and even concrete. Applications such as weapon detection and through-wall imaging system deployed in industrial have created the interest of microwave imaging in biological tissues [3][4]. Studies on microwave imaging for brain stroke, brain injuries, and breast cancer detection had been carried out in recent years [5][6].

Recently, a helmet like the structure of 10 triangular patch antenna of experimental microwave setup for brain stroke diagnosis has been built to distinguish between the ischemic and hemorrhagic stroke [7]. Microwave imaging manifest as a convincing technique for biomedical applications as a map of electromagnetic wave scattering is created, resulting from the contrast in the dielectric properties of different tissues. MWI made use of the dielectric properties of the biological tissue for cancer detection as the differences between relative permittivity of healthy tissue and malignant tissues are distinct [8][9]. The dielectric difference between a tumour and white matter can achieve approximately 1.6:1 while for the conductivity is approximately 2:1[10]. Mapping of the scattered energy properties is used to determine the position of a tumour. This research aims to propose the simplest microwave imaging system for brain tumour diagnosis and determine the desired frequency to compromise between the penetration depth and spatial resolution of the image.

II. METHODOLOGY

A. Simulation Setup

A head phantom with different thickness of the tissues is constructed based on [11] as illustrated in Figure 1. The brain size is taken according to the Zubal head phantom slide 36 [12] which is approximately 150 mm x 200 mm. An elliptically shaped of a tumour 32 mm x 40 mm is studied. Since the frequency plays a crucial role in wave penetration, frequency from 0.5 GHz to 4.0 GHz is simulated. The transmission power is limited to 1mW or 0dBm for the radiation and thermal safety [13][14]. The dielectric properties of a brain tumour and the body tissues are taken from [15][20]. The dielectric properties of different brain tissues are tabulated in Table 1. Minimum of eight rectangular patch electrode is deployed in the system for high sensitivity and fast.'

B. Finite Element Modelling

In this study, 2-D finite element model simulation is carried out to prove the proposed methodology in a time efficient way. Finite Element Modelling (FEM) is employed in the study to compute the electric field scattering at the receiving point in the frequency domain.

FEM convert the Helmholtz vector wave equation as given in (1), into a linear system to calculate the electric field values scattered for each of the eight sensing electrodes.

$$\nabla \times \mu_r^{-1}(\nabla \times \vec{E}) - k_0^2\left(\varepsilon_r - \frac{j\sigma}{\omega\varepsilon_0}\right)\vec{E} = 0 \quad (1)$$

where $\mu_r$is the relative permeability (H/m), ε_r the relative permittivity (F/m), ω the angular frequency (rad/s), σ the electric conductivity [S/m], and $k_0^2=\omega\sqrt{\mu_0\varepsilon_0}$ the free-space wave number (m^{-1}).

Eight rectangular sensing electrodes are arranged in an elliptical array around the head phantom where each one of the electrode act as role as transmitting the wave and the remaining seven electrodes is in receiving mode. The electrode generates the electric field perpendicular to the transverse plane of the head causing Transverse Magnetic (TM) polarisation. The Perfect Electric Conductor (PEC) is applied to correspond with an electrical field where all tangential components are zero [16].

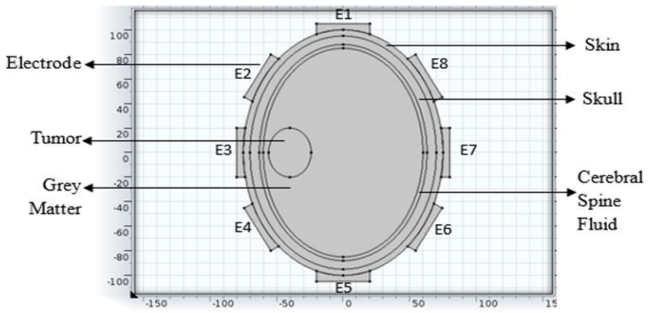

Figure 1: Brain cross-sectional geometry consisting of a brain tumour with a radius of 16mm x 20mm, skin, skull, Cerebral Spinal Fluid (CSF), grey matter from outmost layer to the inmost layer.

Table 1
Dielectric Properties of Brain Tumour at 1 GHz [15] [20]

Tissue	Relative permittivity,ε_r	Conductivity, σ [S/m]
Skin	41	0.89977
Bone	12	0.15566
Cerebral Spine Fluid	68	2.4552
Grey Matter	52	0.98541
Tumour	62.5	1.2438

C. Linear Back Projection

Image reconstruction algorithm of microwave imaging is a numerically nonlinear and ill-posed scattering problem. Contrast Source Inversion (CSI) and Gauss-Newton Inversion (GNI) are commonly being applied for solving the non-linear inversion [12].

To achieve fast computation and less complexity in the system, the brain image is reconstructed using Linear Back Projection (LBP) [17]. The image reconstruction algorithm utilises transmitted and scattered electromagnetic fields information obtained from forwarding problem solution.

The contrast between the scattered energy of electric field without phantom and electric field with phantom is computed by using the Root Mean Square Error (RMSE) to increase the accuracy for the detection and localisation of a tumour [18][19].

In LBP algorithm, the computed sensitivity maps from each sensor are combined with the projection data from each sensor. The modelled sensitivity matrices are used to represent the image plane for each view. The mathematical equation for LBP is shown in Equation (2).

$$\boldsymbol{V}_{LBP\,(x,y)} = \sum_{Tx=1}^{8}\sum_{Rx=1}^{8}\boldsymbol{S}_{Tx,Rx} \times \boldsymbol{M}_{Tx,Rx}(x,y) \quad (2)$$

III. Results and Discussion

A. Evaluation of Frequency Response

Different frequency range is applied to observe the change in an electric field as the dielectric properties are frequency dependence. An appropriate frequency needs to be chosen to compromise the image quality and penetration depth. Figure 2 shows the simulation of a brain tumour at the left side of the brain (x=-40mm, y=0mm) in the frequency range of 0.5GHz to 4GHz.

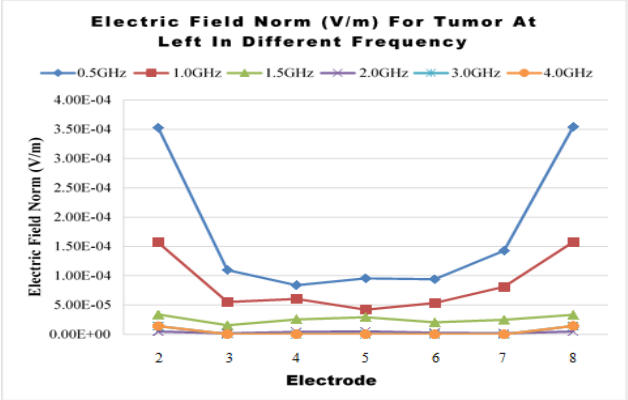

Figure 2: Brain tumour on the left side of the brain (x=-40mm, y=0mm) in the frequency range of 0.5GHz to 4GHz.

Based on Figure 2, the electric field strength receives by the electrodes decrease as the frequency increase. This explains that when the frequency increases the attenuation increase as the material absorb most of the energy.

As the increase in frequency, the relative permittivity decreases while the conductivity of the tissue increases. This can be explained in Equations (3) and (4). The conductivity determines the electrical losses as an attenuation. The conductivity increase will lead to an increase in attenuation. Hence great attenuation occurs as the energy is mostly absorbed by the tissue when high frequency is applied.

The dielectric properties of a tissue can be determined by measuring the complex relative permittivity, ε of the material, defined as:

$$\varepsilon = \varepsilon' - j\varepsilon'' \quad (3)$$

where ε' , represents the relative permittivity, j=√-1 and $\varepsilon''$is dielectric loss coefficient and can be written as:

$$\varepsilon'' = \sigma/(\varepsilon_o)\omega \quad (4)$$

As it is indicated in (4), the loss factor is a function of conductivity and frequency. Also, ε_o and ω represent the permittivity of free space and angular frequency of the field respectively. While σ represents the electric conductivity [S/m], ε_o is indicated in farads per meter (F/m) and ω in radians per second (rad/sec).

Best frequency is selected from the range of 0.5 GHz to 1.5GHz as the electric field after 1.5 GHz is almost equal to zero. To compromise the image quality and penetration depth, 1 GHz is chosen.

The image is reconstructed in different frequency to examine the quality of the image. Table 2 is the images obtain from the simulation at a different frequency.

Table 2
Reconstruction of Brain at Frequency from 0.5GHz to 2GHz

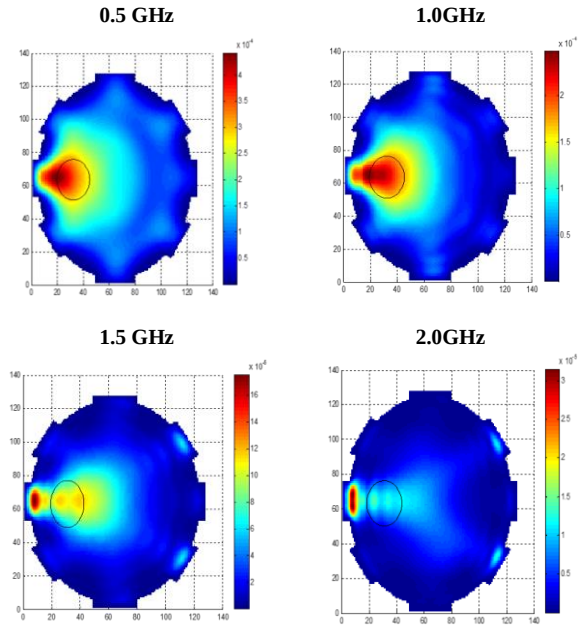

According to the Table II, for frequency from 0.5 GHz to 1.0 GHz, the increase in frequency gives more energy for the microwave to interact with tissue and produce strong scattering. However, the frequency greater than 1.0 GHz and onward, the image quality decrease as the increase in frequency, the attenuation increase, and signal captured by the receiving sensor is reduced. As a conclusion, 1.0GHz is the best frequency for brain tumour detection based on the graph and image constructed.

B. Evaluation of Tumor Position

An elliptically shaped tumour of radii 16 and 20 mm is inserted at a different position to examine the reliability of the system. Figure 3 to Figure 8 is the comparison of the electric field with a tumour and without a tumour.

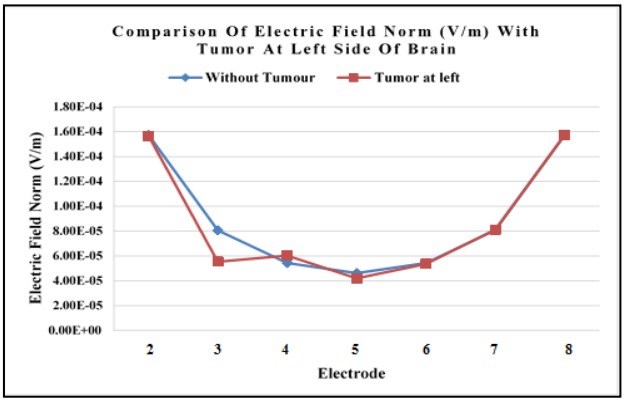

Figure 3: Comparison Electric Field Norm (V/m) with Tumor at the left side of the brain. (x=-40mm, y=0mm)

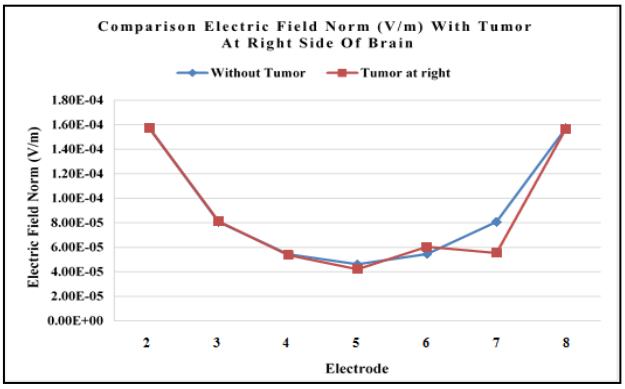

Figure 4: Comparison Electric Field Norm (V/m) with Tumor right side of the brain. (x=-40mm, y=0mm)

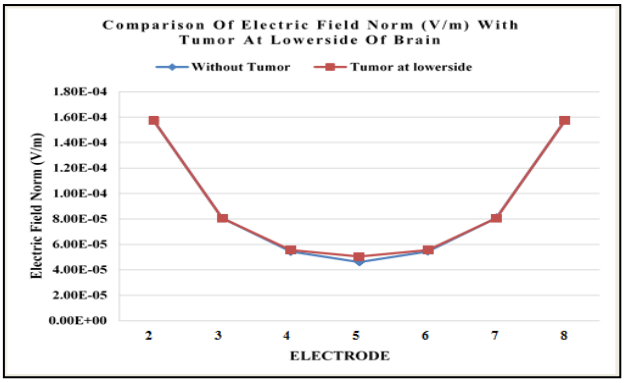

Figure 5: Comparison Electric Field Norm (V/m) with Tumor at the lower side of the brain. (x=-0mm, y=-60mm)

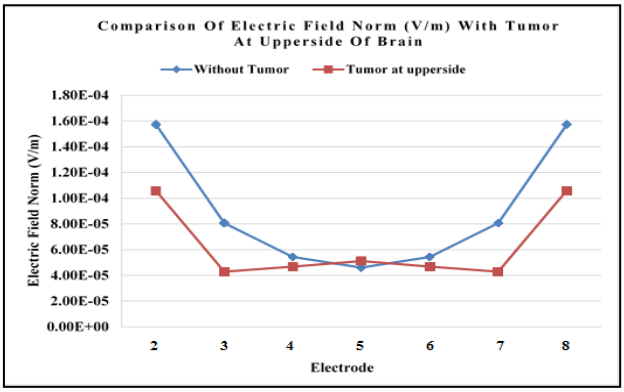

Figure 6: Comparison Electric Field Norm (V/m) with tumour at the upper side of the brain. (x=-0mm, y=60mm)

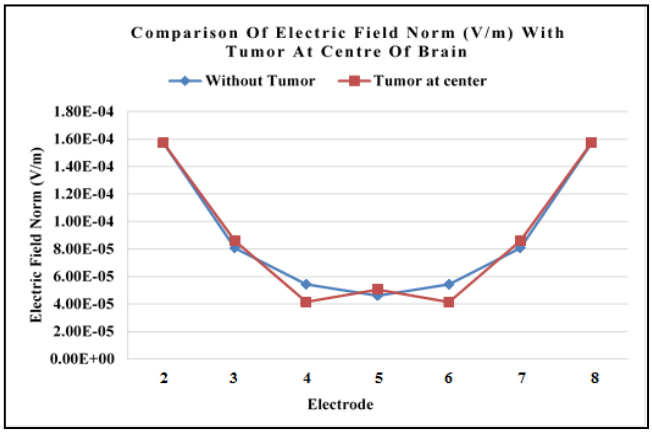

Figure 7: Comparison Electric Field Norm (V/m) with Tumor at the centre of the brain. (x=-0mm, y=0mm)

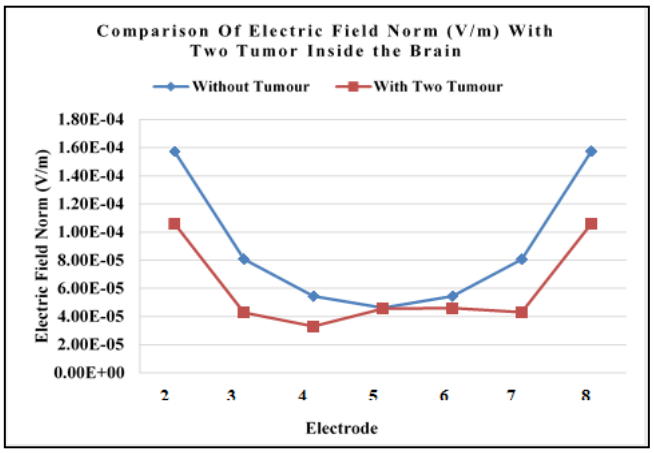

Figure 8: Comparison Electric Field Norm (V/m) with two tumours inside the brain. (x=-30mm, y=-40mm) and (x=0mm, y=60mm)

From Figure 3 to Figure 8, the electric field strength reduces greatly when a tumour is present in the brain. As the tumour is inserted at the left side of the brain near the electrode no.3, the electric field received by the electrode is reduced as energy lost when penetrating through the tumour. Same goes to the tumour at the right near the electrode no.7, the electric field captured by the electrode no.7 is greatly reduced.

Electric field norm varies in all the receiving electrode when a tumour is located at the front part of the brain. This is due to the position of the tumour is nearer to the point source and causing strong scattering. In Figure 5, the electrode no.5 show the changes in an electric field which mean there is a tumour in the lower part of the brain. Lastly, the tumour located at the deep centre of the brain changes the electric field at the electrode no. 2, 3,4,5,6, and 7. The system is further tested by inserting two tumours inside the brain. As a brain tumour is a highly lossy medium, when microwave penetrates through a tumour, attenuation and the strong scattering energy is produced. As a conclusion, the system can detect a tumour at a different position in 1.0 GHz

The image for a tumour (32mm x 40mm) at a different position is reconstructed. Table 3 demonstrates the image of tumour position reconstruction.

Table 3
Reconstruction of Brain Phantom with Tumour at Different Position in Frequency of 1GHz

X=0 mm, Y=60mm	**Front Part**
X=0mm,Y=0mm	**Center**
X=-40mm, Y=0mm	**Left**
X=-30mm, Y=-40mm and X= 0mm, Y=60mm	**Two Tumor**

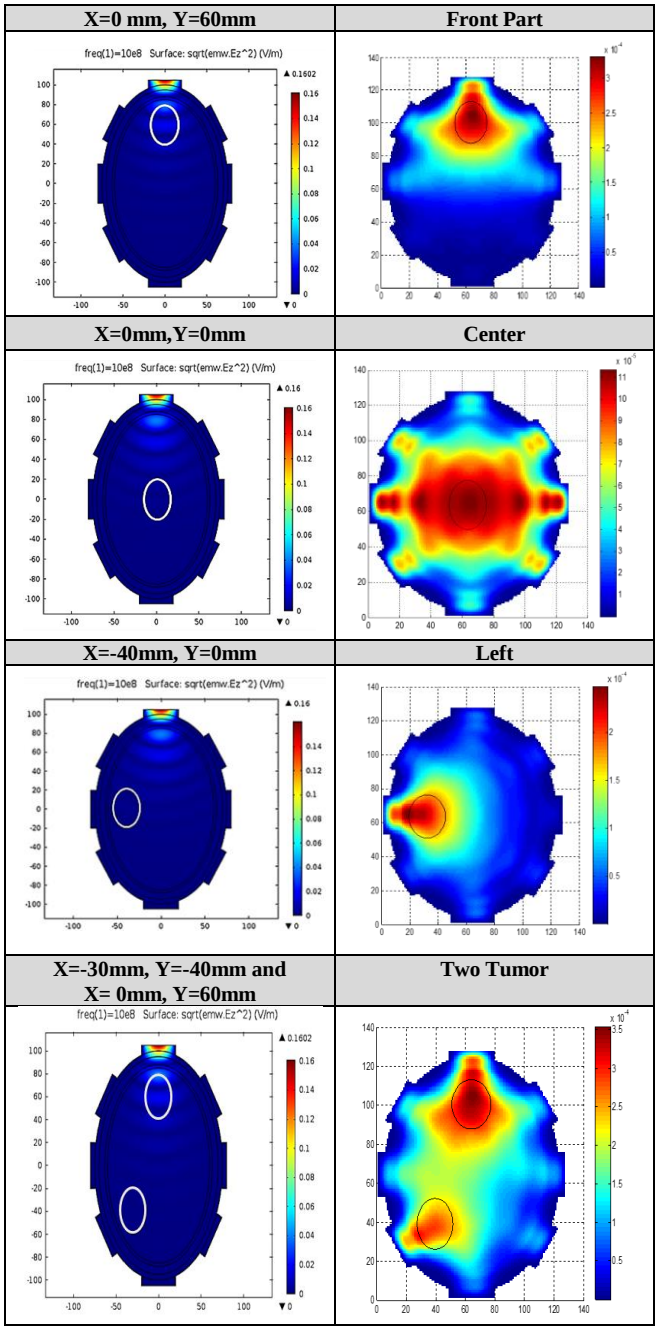

C. Evaluation of Size of Tumour

Despite position, the different size of the tumor has been simulated to evaluate the sensitivity of the system. The tumour is inserted at the position x=-40mm, y=0mm with different size. The size of tumor includes 32mmx40mm, 20mm x 30mm and 10mm x 20mm. Figure 9 illustrates the different electric field norm when a different size of the tumor is simulated.

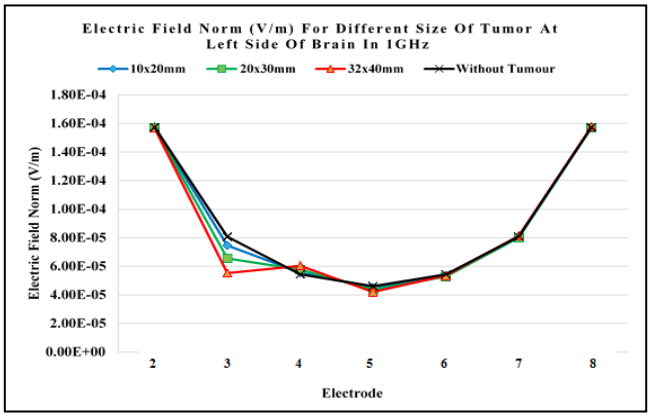

Figure 9: Electric Field Norm (V/m) for Different Size of Tumour at the left side of the brain in 1GHz.

Based on Figure 9, the system can detect a tumour as small as 10x20mm. As the size of the tumour increase the attenuation increase. Hence there is the large difference at the electrode no.2 for tumour size 32x40mm. Besides, that is, the bigger the tumour, the stronger the scattering produce. As the tumour size decrease, the difference between the electric field received by the electrode is reduced.

Table 4 shows the image reconstructed of tumours with different size in frequency 1.0 GHz at position (x=-40mm, y=0mm). Based on images reconstructed, the bigger the tumour the contrast of electric field norm between brain phantom without a tumour and with a tumour is large. Hence easier for the system to localise a tumour and estimate its size. This system can successfully detect the existence of a tumour as small as 10mm x 20mm although it shows difficulties in estimating the size of a tumour. Weak scattering produced by the small tumour increase the complexity for size estimation.

IV. CONCLUSION

Microwave Imaging system by using eight rectangular patch electrodes surrounded by the brain can detect the brain tumour successfully. In conclusion, the objectives have been achieved. By using the Finite Element Analysis, the scattered electric field can be calculated, and the sensitivity map for each projection has been developed. Data of sensitivity map and electric field strength are then exported, and 2D images of the tumour and brain tissue cross are reconstructed using linear back projection.

The analytical results presented in this project proved that changes in the electric field strength due to the presence of a tumour could detect the tumour size as small as 10 mm x 20mm at a frequency of 1 GHz. Based on the plotted graph and the image reconstructed, 1GHz has proven as the most suitable frequency for microwave sensing and imaging for a brain tumour.

In short, the proposed model provides a good direction for further research of more advanced imaging modalities in the medical field. Thus, a new potential technique that is not only non-invasive but is also functional in a contactless environment with the patient is seen in MWI based technique

Table 4
Reconstruction of Brain Phantom with Tumour with Different Sizes in Frequency of 1GHz

Diameter	32x40mm
Diameter	20x30mm
Diameter	10x20mm

ACKNOWLEDGEMENT

The authors are grateful for the funding from the Ministry of Higher Education Malaysia under FRGS Grant (FRGS/1/2015/WAB07/UNIMAP/02/1).

REFERENCES

[1] K. J. Johnson, J. Cullen, J. S. Barnholtz-Sloan, Q. T. Ostrom, C. E. Langer, M. C. Turner, R. McKean-Cowdin, J. L. Fisher, P. J. Lupo, S. Partap, J. A. Schwartzbaum, and M. E. Scheurer, "Childhood brain tumor epidemiology: A brain tumor epidemiology consortium review," *Cancer Epidemiol. Biomarkers Prev.*, vol. 23, no. 12, pp. 2716–2736, 2014.

[2] J. D. Mathews, A. V Forsythe, Z. Brady, M. W. Butler, S. K. Goergen, G. B. Byrnes, G. G. Giles, A. B. Wallace, P. R. Anderson, T. A. Guiver, P. McGale, T. M. Cain, J. G. Dowty, A. C. Bickerstaffe, and S. C. Darby, "Cancer risk in 680,000 people exposed to computed tomography scans in childhood or adolescence: data linkage study of 11 million Australians," *Bmj*, vol. 346, no. May, p. f2360, 2013.

[3] N. Petrović, "Measurement System for Microwave Imaging Towards a Biomedical Application," 2014.

[4] L. Guo and A. M. Abbosh, "Microwave Stepped Frequency Head Imaging Using Compressive Sensing With Limited Number of Frequency Steps," *IEEE Antennas Wirel. Propag. Lett.*, vol. 14, no. 1, pp. 1133–1136, 2015.

[5] M. Persson, A. Fhager, H. D. Tréfna, P. Takook, Y. Yu, T. McKelvey, J. E. Karlsson, X. Zeng, H. Zirath, and M. Elam, "Microwave based diagnostics and treatment in practice," in *2013 IEEE MTT-S International Microwave Workshop Series on RF and Wireless Technologies for Biomedical and Healthcare Applications, IMWS-BIO*

2013 - Proceedings, 2013, pp. 0–2.

[6] A. Fhager, H. D. Trefna, P. Takook, Y. Yu, T. McKelvey, J.-E. Karlsson, X. Zeng, M. Elam, H. Zirath, and M. Persson, "Microwave technology in medical diagnostics and treatment," in *2015 IEEE MTT-S 2015 International Microwave Workshop Series on RF and Wireless Technologies for Biomedical and Healthcare Applications (IMWS-BIO)*, 2015, pp. 133–134.

[7] X. Wan, D. Yang, M. Cai, S. Han, S. Wu, and W. Hao, "The latest research status and prospect on microwave technology for monitoring concerned brain activity," in *2015 IEEE International Conference on Mechatronics and Automation, ICMA 2015*, 2015, pp. 297–302.

[8] S. Y. Semenov and D. R. Corfield, "Microwave Tomography for Brain Imaging: Feasibility Assessment for Stroke Detection," *Int. J. Antennas Propag.*, vol. 2008, pp. 1–8, 2008.

[9] C. Gabriel, R. W. Lau, and C. Gabriel, "The dielectric properties of biological tissues: III. Parameteric models for the dielectric spectrum of tissues," *Phys. Med. Biol.*, vol. 41, pp. 2271–2293, 1996.

[10] S. M. Yacoob and N. S. Hassan, "FDTD analysis of a noninvasive hyperthermia system for brain tumors," *Biomed. Eng. Online*, vol. 11, no. 1, p. 47, 2012.

[11] N. Priyadarshini and E. R. Rajkumar, "Finite Element Modeling of scattered electromagnetic waves for stroke analysis," *Annual International Conference of the IEEE Engineering in Medicine and Biology Society*, vol. 2013, no. 1, pp. 2404–2407, 2013.

[12] A. Munawar, Z. Mustansar, and A. Maqsood, "Analysis of Microwave Scattering from a Realistic Human Head Model for Brain Stroke Detection Using Electromagnetic Impedance Tomography,"*Progress In Electromagnetics Research*, vol. 52, no. November, pp. 45–56, 2016.

[13] A. T. Mobashsher and A. M. Abbosh, "Developments of Tomography and Radar-based Head Imaging Systems," 2015.

[14] A. T. Mobashsher, K. S. Bialkowski, A. M. Abbosh, and S. Crozier, "Design and experimental evaluation of a non-invasive microwave head imaging system for intracranial haemorrhage detection," *PLoS One*, vol. 11, no. 4, pp. 1–29, 2016.

[15] D. S. Yoo, "The dielectric properties of cancerous tissues in a nude mouse xenograft model," *Bioelectromagnetics*, vol. 25, no. 7, pp. 492–497, 2004.

[16] M. Naseri, "Microwave Tomography for Breast Cancer Detection," Chalmers University Of Technology, 2015.

[17] M. Soleimani, "Computational aspects of low frequency electrical and electromagnetic tomography: A review study," *Int. J. Numer. Anal. Model.*, vol. 5, no. 3, pp. 407–440, 2008.

[18] M. Jalilvand, C. Wu, J. Schmid, and T. Zwick, "Quantitative imaging of numerically realistic human head model using microwave tomography," *Electron. Lett.*, vol. 50, no. 4, pp. 255–256, 2014.

[19] F. Yang, Y. Chen, R. Wang, and Q. Zhang, "Super-resolution Microwave Imaging : Time-domain Tomography using Highly Accurate Evolutionary Optimization Method," in *In Antennas and Propagation (EuCAP), 2015 9th European Conference on*, 2015, no. 2, pp. 1–4.

[20] Federal Communications Commision "Dielectric properties of Body Tissues at RF and Microwave Frequencies", on-line http://www.fcc.gov/fcc-bin/dielec.sh